CHAPTER VI

EFFECT OF THE SURFACE TOPOGRAPHY OF ELECTROSPUN POLY(ε-CAPROLACTONE)/POLY(3-HYDROXYBUTYRATE-*CO*-3-HYDROXYVALERATE) FIBROUS SUBSTRATES ON CULTURED BONE CELL BEHAVIOR

6.1 Abstract

The use of electrospun fibrous matrices as substrates for cell/tissue culture has usually been confined to those constituting of smooth fibers. Here, we demonstrated that *in vitro* responses of mouse calvaria-derived, pre-osteoblastic cells (MC3T3-E1) that had been cultured on the electrospun fibrous substrates made from the blend solutions of 50/50 w/w of poly(ε-caprolactone) (PCL) and poly(3-hydroxybutyrate-*co*-3-hydroxyvalerate) (PHBV) of varying concentrations, ranging from 4 to 14 wt%, depended strongly on the topography of the individual fibers. As the concentration of the blend solutions increased from 4 to 14 wt%, the topography of the individual fibers changed from discrete beads/smooth fibers, to beaded fibers/smooth fibers, and finally to smooth fibers and the average diameter of the individual fibers increased from ~0.4 to ~1.8 μm. The results clearly showed that MC3T3-E1 preferred the smooth and hydrophilic surface of the fibrous substrate from 10 wt% PCL/PHBV solution, as the cells appeared to attach, proliferate, and differentiate on the surface of this substrate particularly well.

(**Key-words**: Electrospun fibrous substrates; PCL; PHBV; Bone cell)

6.2 Introduction

The replacement of a large bone defect (i.e., the defect with the size that is beyond the ability of the bone tissue to self-regenerate) requires the use of a scaffold with a three-dimensional porous structure that favors the infiltration of bone cells and new blood vessels. The material used in the fabrication of the scaffold should be biocompatible and exhibit the rate of degradation that is comparable to that of the

neo-tissue. It should also exhibit mechanical properties that are suitable for maintaining the integrity of the replaced site throughout the course of the healing process. Furthermore, high porosity and suitability of topography and chemical functionality of the surface of the scaffold are important factors determining its effectiveness when it is in contact with biological entities in the replaced site (Thomson, 1995; Tuzlakoglu, 2005; Kenar, 2006).

Among various types of scaffolds, the ones exhibiting a fibrous architecture resembling the fibrillar structure of the natural extracellular matrix (ECM) of the connective tissues showed much better support for the attachment and proliferation of the cultured bone cells, when comparing with those of smoother surface (e.g., films) (Wutticharеonmongkol *et al.*, 2006). Various techniques that have been used to fabricate fibrous scaffolds are, for examples, phase separation, melt blowing, and electrospinning (Wutticharеonmongkol, 2006; Zhang, 2005; Li, 2002). Low tooling costs, technical simplicity, and numerous unique characteristics of the obtained fibrous materials (e.g., small diameters of the individual fibers ranging from tens of nanometers to few micrometers, inter-connected porous structure of the obtained matrices, and vast possibilities for surface functionalization) make electrospinning as one of the most commonly utilized fabrication methods of fibrous matrices for biomedical applications (Taepaiboon, 2006; Noh, 2006; Kenawy, 2003). However, the use of the fibrous matrices as substrates for cell/tissue culture has, thus far, been confining to those consisting mainly of smooth individual fibers (Tuzlakoglu, 2005; Noh, 2006; Kenawy, 2003). It is known that morphology of the individual, electrospun fibers is most affected by the variation in the concentration, hence the shear viscosity, of the spinning solutions (Deitzel *et al.*, 2001). As the shear viscosity increases, the morphology of the obtained products would change from discrete droplets, to beaded fibers, and finally to smooth fibers of varying cross-sectional shapes (i.e., round, ribbon-like, etc.). Additionally, the size of the individual fibers (for beaded and smooth fibers) increases monotonically with an increase in the shear viscosity of the spinning solutions (Deitzel *et al.*, 2001). Since beads have usually been considered as defects of the fibers (i.e., for beaded fibers), proposed uses of the electrospun products in biomedical applications have been confining to those constituting of smooth fibers (Wutticharеonmongkol, 2006; Kenawy, 2003). The

main objective of the present work is therefore to investigate the biological response of mouse calvaria-derived, pre-osteoblastic cells (MC3T3-E1) that are cultured on electrospun fibrous substrates with varying surface topographies of the individual fibers.

Among the various biocompatible and biodegradable materials that have usually been fabricated as bone scaffolds, poly(ε-caprolactone) (PCL), poly(3-hydroxybutyrate-*co*-3- hydroxyvalerate) (PHBV), their blends and the blends of each of them with another biocompatible and biodegradable polymer [e.g., poly(3-hydroxybutyrate) (PHB), polylactide (PLA), etc.], and their composites with an osteoconductive material [e.g., hydroxyapatite (HAp)] have been shown to provide very good support for the attachment, proliferation, and differentiation of the cultured bone cells (Chuenjitkuntaworn, 2010; Sombatmankhong, 2006; Ito, 2005). PCL, a US food and drug administration (USFDA)-approved material for craniofacial indications, is a synthetic semi-crystalline aliphatic polyester, with low glass transition and melting temperatures (Ndreu and Yeo, 2008). The popularity of PCL as bone scaffolding material stems from its solubility in a wide range of common organic solvents, its non-toxic biodegradation products, and the degradation rate that is suitable for harboring the bone regeneration (Bölgen *et al.*, 2005). Various forms of PCL, such as electrospun fibrous scaffolds (Wutthichareonmongkol *et al.*, 2006), particulate-leached porous scaffolds (Chuenjitkuntaworn *et al.*, 2010), centrifugation-induced porous scaffolds (Oh *et al.*, 2007), spiral- structured porous scaffolds (Wang *et al.*, 2010), and porous scaffolds made by precision-extruding deposition (PED) method (Shor *et al.*, 2009), have been shown to provide good support for bone regeneration *in vitro* and/or *in vivo*. On the other hand, PHBV, the most common copolymeric variant of PHB, is a semicrystalline aliphatic polyester produced naturally in certain strains of bacteria (Holmes, 1985; Gassner, 1996; Sudesh, 2000). PHB is ideal to be used *in vivo*, since its biodegradation product, D,L-β-hydroxybutyrate (HB), is a normal component of blood and tissues (Cheng *et al.*, 2006). Notwithstanding, PHBV is most utilized, due mainly to the presence of hydroxyvalerate comonomeric unit that reduces the crystallinity and, simultaneously, improves flexibility and processability (Sudesh *et al.*, 2000). PHBV, in various forms, such as electrospun fibrous scaffolds (Sombatmankhong *et al.*, 2006) and

particulate-leached porous scaffolds (Rivard *et al.*, 1996), have been shown to provide good support for the growths of various cell types, including osteoblasts, fibroblasts, Schwann cells, epithelial cells, and ovine chondrocytes.

In this work, fibrous substrates of varying surface topographies of the individual fibers were prepared by electrospinning from the blend solutions of 50/50 w/w PCL/PHBV in a mixture of chloroform and *N,N*-dimethylformamide (DMF). This was achieved through the variation of the concentration of the solutions (i.e., between 4 and 14 wt%). The effect of the solution concentration on the morphology of the individual fibers as well as the morphology, mechanical integrity, and the physico-chemical properties of the obtained fibrous scaffolds was examined in comparison with those of the fibers obtained from solutions of the individual polymeric constituents. The potential for use of these fibrous matrices as bone scaffolds was assessed *in vitro* with MC3T3-E1, in terms of the attachment, proliferation, alkaline phosphatase (ALP) activity, and mineralization.

6.3 Experimental

6.3.1 Materials

Poly(ε-caprolactone) (PCL; M_w = 80,000 g·mol^{-1}) and poly(3-hydroxybutyrate-*co*-3-hydroxyvalerate) (PHBV; M_w = 680,000 g·mol^{-1}) were purchased from Sigma-Aldrich, USA. *N,N*-dimethylformamide (DMF), dichloromethane (DCM), and chloroform were purchased from Labscan (Asia), Thailand. All other chemicals were analytical reagent grade and used without further purification.

6.3.2 Preparation of Fibrous Substrates

Blend solutions of 50/50 w/w PCL/PHBV of varying concentrations ranging from 4 to 14 wt% were prepared in 80/20 v/v chloroform/DMF at room temperature (25 ± 1 °C). PCL solution at 12 wt% was prepared in 50/50 v/v DCM/DMF at room temperature and PHBV solution at 14 wt% was prepared in chloroform at 50 °C (Sangsanoh *et al.*, 2007). Electrospinning of these solutions was

carried out using a typical method. Briefly, each of the solutions was contained in a glass syringe, the open end of which was connected to a gauge-20 stainless steel needle (o.d. = 0.91 mm), used as the nozzle. An aluminum (Al) sheet wrapped around a rotating drum (width and o.d. of the drum ~ 15 cm; rotational speed ~ 50 rpm) was employed as a collector. The distance from the tip of the needle to the outer surface of the Al sheet was set at 10 cm. A Gamma High-Voltage Research D-ES30PN/M692 power supply was used to generate a high DC potential (i.e., 21 kV for the blend and PCL solutions and 12 kV for the PHBV solution). The emitting electrode (+) of the power supply was attached to the needle, while the grounding one was to the collector. A Kd Scientific syringe pump was used to maintain the feed rate of the solution at ~1 $mL \cdot h^{-1}$. The solutions were electrospun consecutively for ~10 h.

6.3.3 Characterization

The viscosities of the polymer solutions were measured by a Brookfield DVIII Ultra rheometer at room temperature and 20 rpm rotational speed of the spindle ($n = 5$).

The surface topographies and sizes of the individual fibers as well as those of the beads (in case of the beaded fibers) of the obtained fibrous substrates were analyzed by a JEOL JSM-5410LV scanning electron microscope (SEM). For each sample, the sizes of the individual fibers (and beads, where applicable) were measured from various positions of at least five different SEM images by SemAphore 4.0 software ($n \geq 50$). Additionally, the thicknesses of the fibrous substrates were measured by a Mitutoyo digital micrometer ($n = 5$).

The chemical integrity of the obtained fibers was identified by a Nicolet NEXUS407 Fourier- transform infrared spectrometer equipped with the attenuated total reflection mode (ATR-FTIR), at a resolution of 4 cm^{-1} over a wavenumber range of 4000 to 400 cm^{-1}.

Static water contact angles of the obtained fibrous substrates were measured by a KRÜSS DSA 100 drop shape analysis system. Ten droplets of distilled water (10 μL) were placed randomly at different positions of each sample. The projected images of the droplets, after they had been allowed to stay on the

substrates until no further change in their shapes was observed, were analyzed for the contact angles, and the data were averaged.

The mechanical integrity, in terms of the tensile strength and Young's modulus, of the obtained fibrous substrates (rectangular shape, 10 mm × 100 mm) was assessed using a Lloyd LRX universal testing machine (gauge length = 50 mm and crosshead speed = 20 mm·min^{-1}) (n = 5).

The true densities of the obtained fibrous scaffolds ($\rho_{scaffold}$) were measured on ~1 g samples using a Quantachrome Ultrapycnometer-1000 gas pycnometer (n = 5). On the basis of the obtained data, porosities and pore volumes of the matrices can be respectively calculated from the following expressions: $(1 - \rho_{scaffold}/\rho_{polymer}) \times 100$ and $(1/\rho_{scaffold} - 1/\rho_{polymer})$, where $\rho_{polymer}$ represents the bulk density of the polymeric constituent(s). Here, ρ_{PCL}, ρ_{PHBV}, and $\rho_{PCL/PHBV(50/50\ w/w)}$ were taken as 1.145, 1.250, and 1.198 g·cm^{-3}, respectively.

6.3.4 Cell Culturing

Mouse calvaria-derived, pre-osteoblastic cells (MC3T3-E1; ATCC CRL-2593) were cultured in minimum essential medium with Earle's Balanced Salts (MEM; HyClone, USA), supplemented by 10% fetal bovine serum (FBS; Biochrom, UK), 1% L- glutamine (Invitrogen, USA), and 1% antibiotic and antimycotic formulation (containing penicillin G sodium, streptomycin sulfate, and amphotericin B; Invitrogen, USA). The medium was replaced on every other day and the cultures were maintained at 37 °C in a humidified atmosphere containing 5% CO_2. Fibrous substrate specimens (circular discs, ~15 mm in diameter) were placed in wells of a 24-well tissue-culture polystyrene plate (TCPS; Corning, USA) and subsequently sterilized in 70% ethanol for 90 min. The specimens were then washed with autoclaved deionized water and then immersed in MEM overnight. A metal ring (~12 mm in diameter) was placed on top of each specimen to ensure a good contact of the specimen with the bottom of each well. MC3T3-E1 from the cultures were trypsinized (0.25% trypsin containing 1 mM ethylenediaminetetraacetic acid (EDTA); Invitrogen, USA), counted by a Hausser Scientific hemacytometer, and

seeded at ~40,000 cells cm^{-2} on each of the specimen and the empty wells of a TCPS (i.e., positive control).

In the attachment and the proliferation studies, cells were cultured in the same media as mentioned above. For other studies, cells were cultured in MEM supplemented by 2% FBS, 1% L-glutamine, and 1% antibiotic and antimycotic during the first 3 d, after which they were cultured in the same medium, but with the addition of an osteogenic supplement [i.e., 5 mM glycerol-2-phosphate disodium salt hydrate (β-glycerophosphate; Sigma-Aldrich, USA) and 50 $\mu g \cdot mL^{-1}$ L-ascorbic acid (Sigma-Aldrich, USA)].

6.3.5 Cell Attachment and Cell Proliferation

The cells were allowed to attach on the fibrous substrate specimens and empty wells of a TCPS for 2, 4, and 6 h in the attachment study (n = 4). At each time point, the number of the attached cells was quantified by a 3-(4,5-dimethylthiazol-2-yl)-2,5-diphenyl-tetrazolium bromide (MTT; Sigma-Aldrich, USA) assay. Additionally, the cells were first allowed to attach on the specimens and empty wells of a TCPS for 16 h, and then measured at 24 h. The number of the proliferated cells was also determined by MTT assay on days 1, 2, and 3 after cell culturing (n = 4). The appearance of the cells during the attachment and the proliferation periods was characterized by SEM (discussed later).

6.3.6 Quantification of Viable Cells (MTT Assay)

MTT assay is a cell quantification method that measures the activity of mitochondria in their ability to reduce a tetrazolium-based compound, MTT, to a purplish formazan product. The amount of purplish formazan product is proportional to the number of viable cells. Each cell-cultured specimen was incubated at 37 °C for 30 min with MTT solution and the formazan product was then dissolved in a mixture of dimethylsulfoxide (DMSO; Carlo Erba, Italy) (900 µL/well) and glycine buffer (pH = 10) (125 µL/well). The absorbance of the supernatant was evaluated with a Thermospectronic Genesis10 UV-visible spectrophotometer at 570 nm. The observed UV absorbance values were converted to the numbers of cells using predetermined standard calibration curves.

6.3.7 Morphological Observation of Cultured Cells

Each cell-cultured specimen, after removal of the culture medium, was rinsed with PBS twice and the cells were then fixed with 3% glutaraldehyde solution (Electron Microscopy Science, USA) at 500 μL/well for 30 min. The specimen was rinsed again with PBS and dehydrated in ethanolic solutions of varying concentrations (i.e., 30, 50, 70, and 90 vol%, respectively) and in pure ethanol for ~2 min each. It was dried in 100% haxamethyldisilazane (HMDS; Sigma-Aldrich, USA) for 5 min and finally in air, after removal of HMDS. The specimens were then observed by SEM and the morphology of the cells that has been cultured on a glass substrate (12 mm in diameter; Menzel, Germany) was used as positive control.

6.3.8 Alkaline Phosphatase (ALP) Analysis

MC3T3-E1 were cultured on the fibrous scaffold MC3T3-E1 were cultured on the fibrous substrate specimens and empty wells of a TCPS for 3 and 7 d to determine ALP activity (n = 4). Each specimen, after removal of the culture medium, was rinsed with PBS. Alkaline lysis buffer (10 mM Tris-HCl, 2 mM $MgCl_2$, 0.1% Triton-X 100, pH 10) (100 μL/well) was added and the specimen was scrapped, sonicated, and then frozen at -20 °C for ~30 min. An aqueous solution of 2 $mg{\cdot}mL^{-1}$ p-nitrophenyl phosphate (PNPP; Invitrogen, USA) mixed with 0.1 M aminopropanol (10 μL/well) in 2 mM $MgCl_2$ (100 μM/well) was added into the specimen, which was then incubated at 37 °C for 30 min. An aqueous solution of NaOH (50 nM at 0.9 mL/well) was added and the extracted solution was measured spectrophotometrically at 410 nm. The amount of ALP was calculated against a predetermined standard curve and then normalized by the amount of total proteins synthesized. For the protein assay, each specimen was treated in the same manner as in the ALP assay up to the point where it was frozen. After freezing, a bicinchoninic acid (BCA; Pierce Biotechnology, USA) solution was added into the specimen and incubated at 37 °C for 30 min. The absorbance of the medium solution was then measured spectrophotometrically at 562 nm, and the amount of the total proteins was calculated against a predetermined standard curve.

6.3.9 Mineralization Analysis

Calcium deposition was investigated by Alizarin Red-S (Sigma-Aldrich, USA) staining. MC3T3-E1 had been cultured on the fibrous substrate specimens and empty wells of a TCPS for 14 d (n = 4), after that the cells were fixed with cold methanol for 10 min, washed with deionized water, and immersed in 1% Alizarin Red-S solution in a mixture of 0.4 mL ammonium hydroxide/40 mL water for 3 min. Each stained specimen was washed several times with deionized water and air-dried at room temperature. The stained specimen was photographed and the redness, signifying the amount of calcium deposition, was quantified by destaining with 10% cetylpyridinium chloride monohydrate (Sigma-Aldrich, USA) in 10 mM sodium phosphate at room temperature for 15 min and spectrophotometically read at 570 nm.

6.3.10 Statistical Analysis

All values were presented as means ± standard deviations. Significance between two data sets was determined by one-way ANOVA analysis, using t-test for all analyses, except for the attachment, proliferation, and ALP activity analytical studies. Scheffe's test was applied to the three studies. The statistical significance was accepted at a 0.05 confidence level.

6.4 Results and Discussion

6.4.1 Characterization of Polymer Solutions and Fibrous Substrates

As previously mentioned, shear viscosity majorly affects the morphology of the individual electrospun fibers (Deitzel *et al.*, 2001). Prior to electrospinning, the PCL/PHBV solutions were measured for the shear viscosities (see Table 6.1). As the total concentration of the blend solutions increased from 4 to 14 wt%, the shear viscosity increased from ~290 to ~580 mPa·s. Electrospinning of these solutions was carried out under the electric field of 21 kV/10 cm (see Figure 6.1 for the representative SEM images of the obtained products). At 4 wt%, a combination of discrete beads (~16 μm on average) and smooth fibers (~0.4 μm on average) was obtained. At 6 and 8 wt%, a combination of beaded and smooth fibers

was evident. At these concentrations, the sizes of the beads were in the range of 2.6–3.4 μm on average, while those of the fibers were in the range of 0.5–0.6 μm on average. The densities of the beads that were observed on the electrospun products of 4, 6, and 8 wt% PCL/PHBV solutions were 1420, 3480, and 3020 beads·mm^{-2} on average, respectively. Between 10 and 14 wt%, only smooth fibers were generated. The size of these fibers increased from ~0.8 μm on average at 10 wt% to ~1.8 μm on average at 14 wt%. It should be mentioned at this point that the blend composition of 50/50 w/w between PCL and PHBV was chosen on the basis of preliminary results, which showed that the fibers that had been obtained from other blend compositions were very nonuniform (results not shown). This may arise from the immiscible of the two polymers (later discussion).

From these SEM images, the individual fibers in all of the fibrous substrates were randomly aligned and they appeared to conglutinate to one another at touching points. While the random alignment related directly to the slow rotational speed of the collection device used during the fiber collection, the partial conglutination was due to the rather short collection distance, hence incomplete evaporation of the solvent from the jet segments during their flights to the collector (Deitzel *et al.*, 2001). Electrospinning of the neat PCL and PHBV solutions was also carried out for comparison (see Figure 6.1). The obtained fibers shared essentially the same features as those from the 10–14 wt% PCL/PHBV solutions. The sizes of these fibers were ~1.0 and ~2.2 μm on average, respectively. Upon consecutive spinning for ~10 h, the thicknesses of the blend fibrous scaffolds ranged between ~90 and ~110 μm on average, while those of the PCL and the PHBV counterparts were ~120 and ~90 μm on average, respectively. The actual sizes of the fibers and beads, where applicable, are also summarized in Table 6.1.

Table 6.1 Viscosities of PCL/PHBV, PCL, and PHBV solutions as well as physical and physico-chemical characteristics of the obtained electrospun fibrous substrates

Sample	Viscosity (mPa·s)	Fiber Diameter (μm)	Bead size (μm)	Water Contact Angle (deg)
4% PCL/PHBV	292 ± 3	0.44 ± 0.09	15.56 ± 0.95	121 ± 2
6% PCL/PHBV	343 ± 4	0.51 ± 0.03	2.57 ± 0.34	117 ± 1
8% PCL/PHBV	371 ± 3	0.58 ± 0.02	3.36 ± 0.23	106 ± 3
10% PCL/PHBV	434 ± 5	0.77 ± 0.02	-	85 ± 2
12% PCL/PHBV	528 ± 5	1.08 ± 0.06	-	90 ± 1
14% PCL/PHBV	581 ± 7	1.79 ± 0.05	-	99 ± 1
12% PCL	451 ± 3	0.96 ± 0.04	-	103 ± 1
14% PHBV	621 ± 2	2.19 ± 0.07	-	115 ± 3

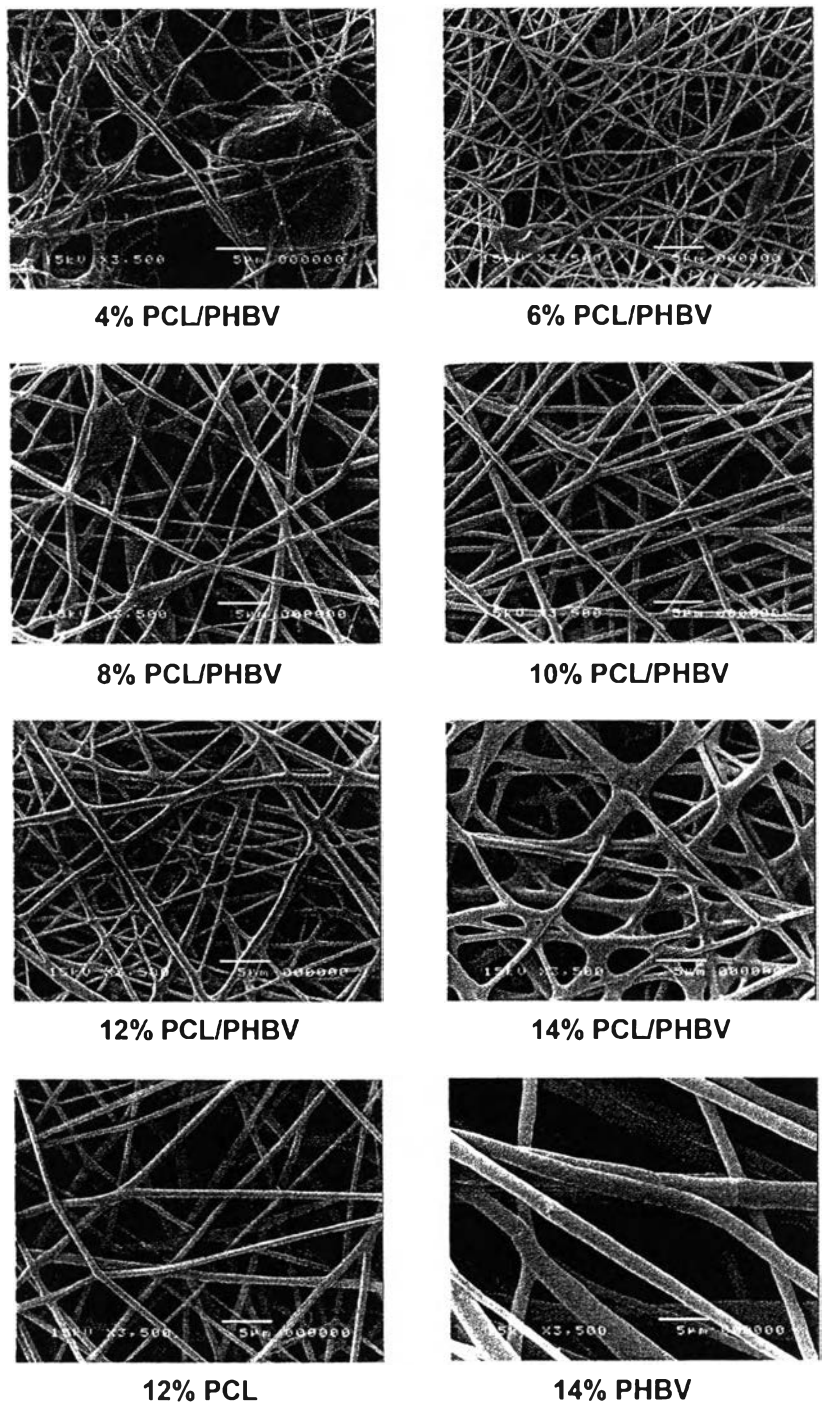

Figure 6.1 Representative SEM images (scale bar = 5 μm and magnification = 3500×) of the electrospun fibrous scaffolds from 4-14 wt% PCL/PHBV, 12 wt% PCL, and 14 wt% PHBV solutions.

The chemical integrity of the PCL/PHBV fibers was investigated by ATR-FTIR (see Figure 6.2). Those of the neat PCL and PHBV counterparts are also shown for comparison. The absorption peak, centering around 1724 cm^{-1}, belonging to the stretching vibrations associated with the crystalline conformations of the carbonyl ester (C=O) (Varnell *et al.*, 1981), was evident in all of the IR spectra. For the blend fibers, the way in which this peak increased in its intensity with an increase in the total concentration of the solutions is indicative of the increase in the total crystallinity. Referring to Figure 6.2, since all of the characteristic peaks of the neat polymers can be observed in the IR spectra of the blend fibers, the existence of both PCL and PHBV components within the blend fibers was confirmed. Furthermore, since no peak shifts and/nor new absorption peaks were observed for the blend fibers, it is expected that specific interactions between PCL and PHBV molecules were inexistent. Qiu *et al.* (2005) showed that solvent-cast PCL/PHBV blend films exhibited distinctive and unchanged glass transition and melting temperatures of either component, which is indicative of an immiscible polymer blend.

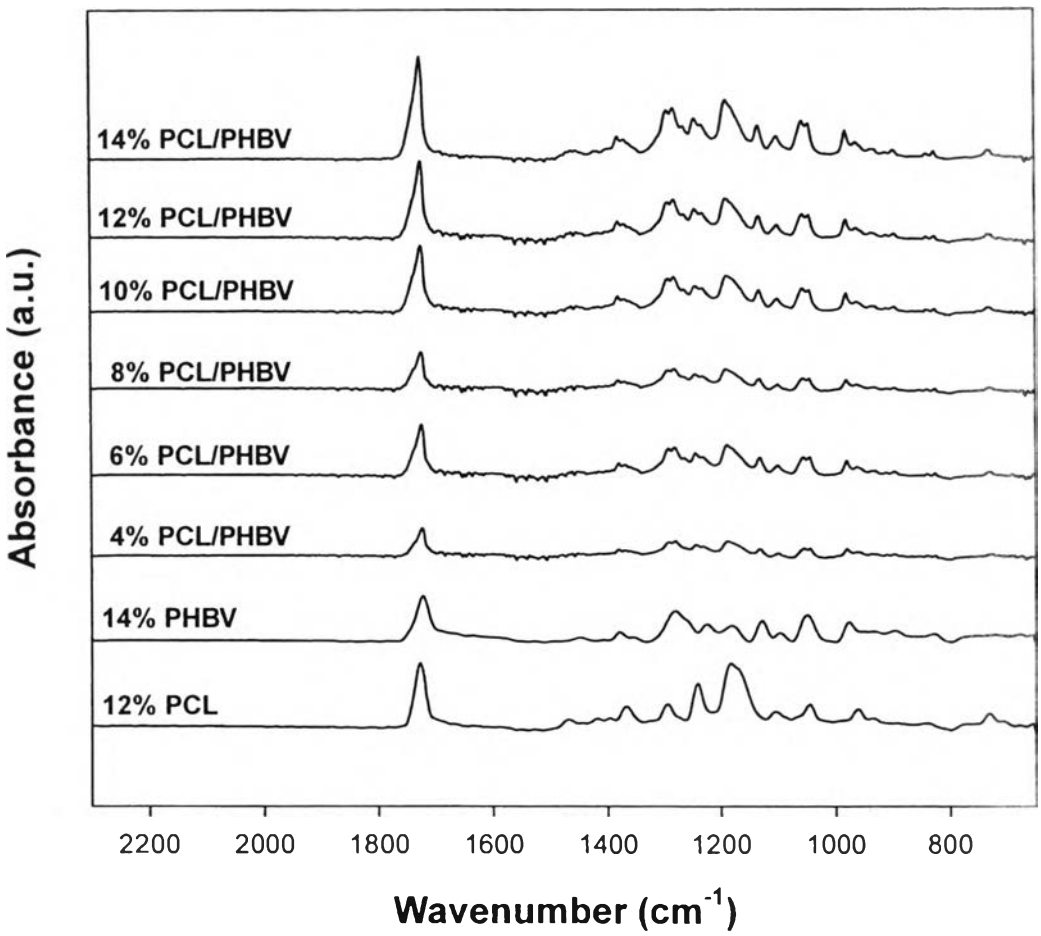

Figure 6.2 ATR-FTIR spectra of the obtained electrospun fibrous scaffolds.

Physico-chemistry, in terms of water contact angles, of all of the fibrous substrates was investigated (see Table 6.1). When the size of the plated water droplet is much greater than those of the underlying fibers of a fibrous substrate, both the size and the topography of the underlying, individual fibers play major roles in controlling the contact angle of the water droplet (Yoon, 2008; Tong, 2011). For the beaded fibers, as the size of the beads decreased (corresponding to the increase in the solution concentration), the water contact angle was found to increase, hence the decrease in the wettability. As the beads disappeared completely (i.e., smooth fibers), a sudden decrease in the water contact angles, hence a sudden increase in the wettability, was observed (Yoon *et al.*, 2008). For the smooth fibers, the increase in the sizes of the fibers was responsible for the observed increase in the water contact

angles, hence the decrease in the wettability (Tong *et al.*, 2011). Here, as the total concentration of the PCL/PHBV solutions increased from 4 to 8 wt%, the average water contact angle of the obtained beaded fibers decreased from ~121 to ~106°. A sharp improvement in the wettability was observed when the smooth fibers were first appeared at 10 wt%, but, as the concentration of the blend solutions increased from 10 to 14 wt%, the average water contact angle of the obtained smooth fibers increased again from ~85 to ~99°. Evidently, the fibrous scaffold that had been obtained from the 10 wt% blend solution exhibited the greatest wettability. Based on the SEM images of the PCL/PHBV fibrous scaffolds in Figure 6.1, it can be postulated that the smoother the surface of the fibrous scaffolds, the better the wettability. For comparison, the water contact angle values of the PCL and the PHBV fibrous scaffolds were ~103 and ~115° μm on average, respectively.

The mechanical integrity in terms of the tensile strength, Young's modulus, and elongation at break of the fibrous scaffolds is also investigated (see Table 6.2). For the blend fibrous substrates, the tensile strength and the elongation at break values were found to increase (i.e., from ~0.98 to ~1.95 MPa on average for the tensile strength and from ~1.4 to ~4.9% on average for the elongation at break), while that of the Young's modulus was found to decrease (i.e., from ~162 to ~103 MPa on average), with an increase in the total concentration of the PCL/PHBV solutions from 4 to 14 wt%. Interestingly, the neat PCL fibrous scaffolds exhibited the greatest values of the tensile strength and the elongation at break (i.e., ~2.41 MPa and ~5.7% on average, respectively) and, at the same time, they showed the lowest value of the Young's modulus (i.e., ~82.4 MPa on average). The property values of the neat PHBV fibrous scaffolds, on the other hand, were relatively moderate (see Table 6.2).

Table 6.2 Mechanical characteristics of the obtained electrospun fibrous substrates

Sample	Tensile Strenght (MPa)	Young's Modulus (MPa)	Elongation at Break (MPa)
4% PCL/PHBV	0.98 ± 0.06	162.1 ± 4.6	1.4 ± 0.2
6% PCL/PHBV	1.21 ± 0.38	145.6 ± 3.7	2.3 ± 0.6
8% PCL/PHBV	1.58 ± 0.17	139.2 ± 3.8	2.8 ± 0.4
10% PCL/PHBV	1.84 ± 0.09	112.3 ± 1.9	4.3 ± 0.7
12% PCL/PHBV	1.87 ± 0.11	108.8 ± 2.2	4.5 ± 0.5
14% PCL/PHBV	1.95 ± 0.26	102.7 ± 2.6	4.9 ± 0.2
12% PCL	2.41 ± 0.36	82.4 ± 5.6	5.7 ± 0.8
14% PHBV	1.79 ± 0.13	126.7 ± 7.1	3.8 ± 0.3

The true densities, porosities, and pore volumes of the obtained fibrous substrates were investigated (see Table 6.3). For the blend fibrous scaffolds, the true density was found to increase (i.e., from ~2.3×10^{-2} to ~3.9×10^{-2} $g \cdot cm^{-3}$ on average), while those of the porosity and the pore volume were found to decrease (i.e., from ~98.1 to ~96.7% on average for the porosity and from ~42.6 to ~24.6 $cm^3 \cdot g^{-1}$ on average for the pore volume), with an increase in the total concentration of the PCL/PHBV solutions from 4 to 14 wt%. The results imply that, as the total concentration of the blend solutions increased, the packing of the underlying fibers also increased. Among all of the fibrous scaffolds investigated, those made of PCL exhibited the lowest porosity value, while those made of PHBV were the greatest (see Table 6.3).

Table 6.3 True densities, porosities, and pore volumes of the obtained electrospun fibrous substrates

Sample	True Density ($\times 10^{-2}$ g·cm^{-3})	Porosity (%)	Pore Volume (cm^3·g^{-1})
4% PCL/PHBV	2.30 ± 0.26	98.1 ± 0.5	42.6 ± 3.2
6% PCL/PHBV	2.61 ± 0.15	97.8 ± 0.3	33.2 ± 2.5
8% PCL/PHBV	2.86 ± 0.54	97.6 ± 0.7	34.1 ± 3.0
10% PCL/PHBV	3.19 ± 0.23	97.3 ± 0.4	30.5 ± 1.7
12% PCL/PHBV	3.57 ± 0.39	97.0 ± 0.7	27.2 ± 1.7
14% PCL/PHBV	3.93 ± 0.38	96.7 ± 0.6	24.6 ± 2.4
12% PCL	4.69 ± 0.11	95.9 ± 0.4	20.6 ± 2.1
14% PHBV	2.13 ± 0.17	98.3 ± 0.2	46.1 ± 2.6

6.4.2 Cell Attachment and Cell Proliferation

Adherence of MC3T3-E1 after having been seeded on the surfaces of TCPS and all types of the fibrous scaffolds for 2, 4, and 6 h is quantitatively shown in Figure 6.3. For any given type of the substrates, the number of the cells increased with an increase in the cell seeding time. At 2 h, the numbers of the cells on the surfaces of almost all types of the fibrous scaffolds, except for those of the scaffolds from 4 wt% PCL/PHBV and 14 wt% PHBV solutions which exhibited significantly lower values, were equivalent to that on TCPS. At 4 h, the numbers of the cells on the surfaces of the fibrous scaffolds from 4, 10, and 12 wt% PCL/PHBV and 12 wt% PCL solutions were equivalent to that on TCPS. At 6 h, only the numbers of the cells on the surfaces of the fibrous scaffolds from 10 and 12 wt% PCL/PHBV solutions were equivalent to that on TCPS. Among the various types of the fibrous scaffolds, the ones from 10 and 12 wt% PCL/PHBV and 12 wt% PCL solutions, regardless of the cell seeding time, appeared to support the attachment of the investigated bone cells slightly better than the others.

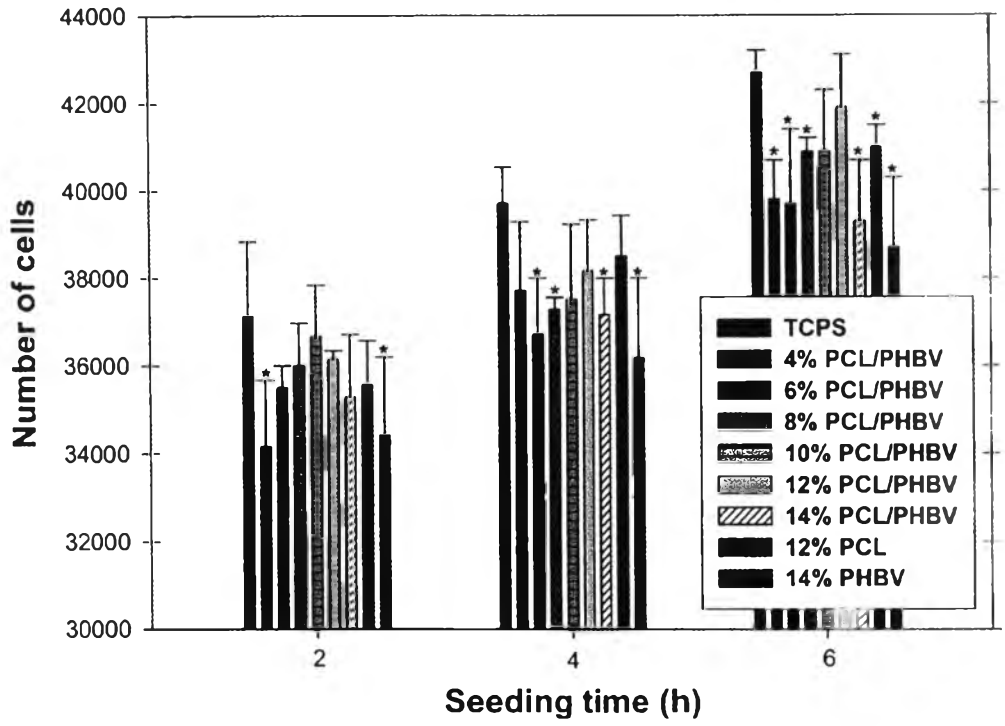

Figure 6.3 Attachment of MC3T3-E1 that were seeded on the surfaces of TCPS and various types of fibrous substrates as a function of cell seeding time. *Significance at $p < 0.05$ with respect to TCPS.

A quantitative analysis of the proliferation of MC3T3-E1 after having been cultured on the surfaces of TCPS and all types of fibrous substrates for 1–3 days is shown in Figure 6.4. For any given type of substrate, the number of the cells increased with an increase in the cell culturing time. On day 1, the numbers of the cells on the surfaces of the fibrous scaffolds from 6-12 wt% PCL/PHBV were equivalent to that on TCPS. On days 2 and 3, the numbers of the cells on the surfaces of the fibrous scaffolds from 6, 10, and 14 wt% PCL/PHBV and 12 wt% PCL solutions were equivalent to that on TCPS. Nevertheless, the average number of the cells proliferated on the surface of the fibrous scaffold from 10 wt% PCL/PHBV solution was greater than those on the surfaces of the other types of the fibrous scaffolds. Particularly on day 3, the average number of the cells on the surface of the fibrous scaffold from 10 wt% PCL/PHBV solution was significantly greater than that of the fibrous scaffold from 12 wt% PCL and slightly greater than that on TCPS.

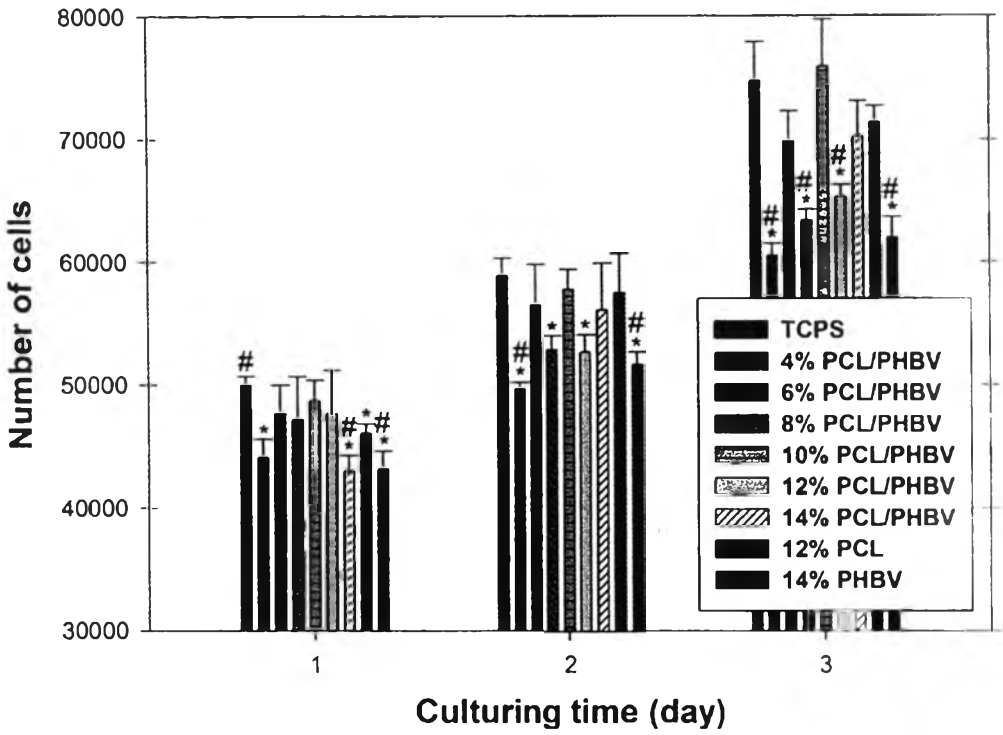

Figure 6.4 Proliferation of MC3T3-E1 that were cultured on the surfaces of TCPS and various types of fibrous substrates as a function of cell culturing time. *Significance at $p < 0.05$ with respect to TCPS. #Significance at $p < 0.05$ with respect to the fibrous substrate from 12 wt% PCL solution.

Though not totally relevant, Kumbar *et al.* (2008) demonstrated that biological response of human skin fibroblasts (hSF) that had been cultured on the surfaces of poly(lactic acid-*co*-glycolic acid) (PLAGA) fibrous scaffolds was, on many aspects, fiber size-dependent. Specifically, the PLAGA fibrous scaffolds with the diameters of the underlying fibers ranging between 250 and 1200 nm showed significantly greater support for the proliferation and the expression of collagen III of the cultured hSF than the matrices with lower or larger fiber diameters. However, no particular trends were observed on the production of collagen I and elastin with the variation in the fiber diameter (Kumbar *et al.*, 2008). Khang *et al.* (1999), prepared poly(*L*-lactide-*co*-glycolide) (PLGA) films with chemogradient wettability by a corona treatment and found that fibroblasts adhered, spread, and grew particularly better onto positions with moderate hydrophilicity (i.e., the water contact angle of

~55°). Based on these studies (Kumbar, 2008; Khang, 1999), both the size of the underlying fibers and hence the wettability of a fibrous scaffold should play important role in mediating the cell behavior. Here, the mouse bone cells appeared to attach and proliferate well on the surface of the fibrous substrate from 10 wt% PCL/PHBV solution, which exhibited the lowest water contact angle of ~85° on average.

Because the adsorption of proteins is influenced by the hydrophilicity/hydrophobicity of a surface, the surface with a certain value of water contact angle would favor the adsorption of certain proteins, which may or may not act as cellular mediators. Additionally, both the size and the topography of the underlying fibers of a fibrous scaffold could influence directly the organization of organelles within the attached cells. Different organizations of the organelles could result in different chemo-signaling pathways that influence directly the cell behavior. While the effect of different surface topographies on wettability, adsorption of proteins, and responses of the cultured bone cells should be a subject of thorough investigations, the effect of different organizations of organelles, in response to difference surface topographies, on certain behaviors of the cultured bone cells can be rationalized from an existing published report (Wang *et al.*, 2011). In an attempt to investigate the effect of fiber alignment on the responses of MG63 human osteosarcoma cells that had been cultured on the surfaces of randomly-aligned and well-aligned poly(L-lactic acid) (PLLA) fibrous scaffolds, Wang *et al.* (2011) found that the cells on the well-aligned fibrous scaffold elongated their cytoplasms along the fiber axis, but they appeared to attach, proliferate, and differentiate better on the randomly-aligned fibrous scaffold. This exemplifies the importance of surface topography of a scaffold on cellular behavior.

Selected SEM images to reveal the morphologies of MC3T3-E1 that had been cultured on the surfaces of glass and all types of the fibrous substrates for various time intervals are shown in Figure 6.5. At 2 h after cell seeding, most of the cells on almost all types of the fibrous substrates were still round, except for those on the surfaces of the fibrous substrates from 6 wt% PCL/PHBV, 10 wt% PCL/PHBV, and 12 wt% PCL solutions that showed slight expansion of their cytoplasms. At this

time point, the cells on the control glass substrate were also still round, but cytoplasmic process in the form of filopodia was clearly visible. At 4 and 6 h after cell seeding, the cells on all types of substrates became more expanded. Interestingly, the cells on the fibrous substrate from 14 wt% PHBV solution were very small and, due to the large size of the individual fibers, appeared to elongate their cytoplasms along the fiber axis. On days 1 and 2 after cell culturing, the cells, in their expanded morphology, proliferated well to cover ~30 to ~40% of the surfaces on almost all of the fibrous substrates. On day 3, full expansion of the cells on all types of the substrates was evidence. Strikingly, the most expansion of the cells was observed for the cells on the fibrous substrate from 10 wt% PCL/PHBV solution, which proliferated to cover ~70% on the surface. Noticeably, the cells on the fibrous substrate from 14 wt% PHBV solution grew in their size, but still exhibited the elongation of their cytoplasms along the fiber axis. Based on the results shown in Figure 6.5, the fibrous substrate from 10 wt% PCL/PHBV solution was clearly the best among the investigated fibrous substrates to support the growth of MC3T3-E1.

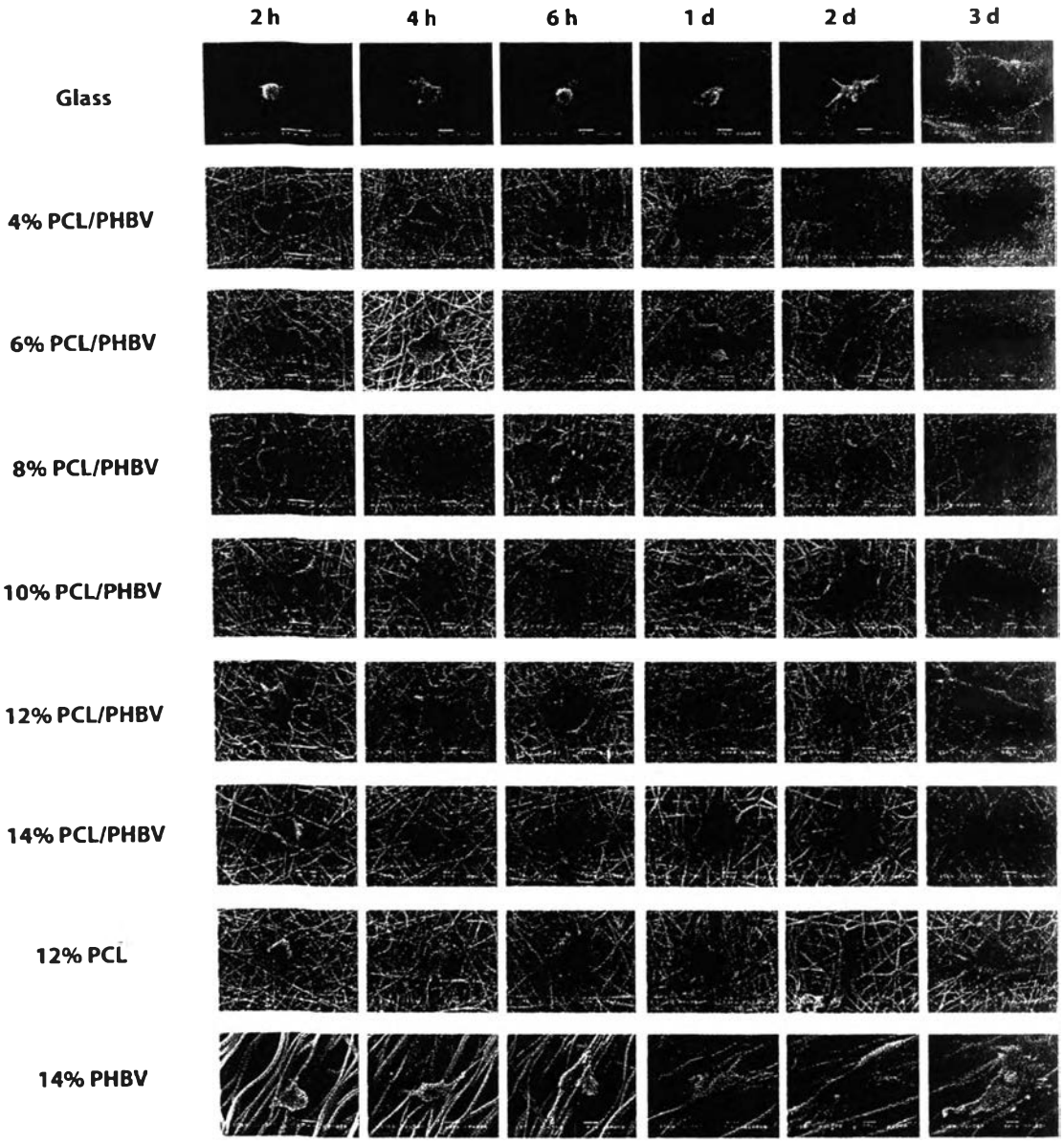

Figure 6.5 Representative SEM images (scale bar = 10 μm and magnification = 1500×) of MC3T3-E1 that were seeded/cultured on the surfaces of a glass substrate (control) and various types of the fibrous substrates at various time points.

6.4.3 Alkaline Phosphatase (ALP) Activity

The expression of ALP from MC3T3-E1 that had been cultured on TCPS and all types of the fibrous substrates for 3 and 7 d is shown in Figure 6.6. On day 3, the ALP activity of the cells that had been grown on the surfaces of TCPS and the fibrous substrates from 6, 10, and 14 wt% PCL/PHBV and 12 wt% PCL solutions

was statistically the same, which appeared to be greater than that of the cells on the rest of the fibrous substrates. On day 7, increases in the ALP activity of the cells that had been grown on all types of substrates was evident. Strikingly, only the cells that had been grown on the surfaces of the fibrous substrates from 10 wt% PCL/PHBV and 12 wt% PCL solutions exhibited the ALP activity in the levels that are statistically equivalent to the cells that had been grown on TCPS, while the cells that had been grown on the surfaces of all other fibrous substrates showed much lower values. Since ALP usually secretes from normal bone cells during the early matrix formation and maturation period and is triggered by cellular contacts (when the cells reached the confluence) and/or by the expression of ample amounts of early matrix proteins (e.g., type I collagen, fibronectin, and/or TGF-β1) (Wutticharconmongkol, 2006; Choi, 1996), it is logical to note that the fibrous substrates from 10 wt% PCL/PHBV and 12 wt% PCL solutions were both able to up-regulate the ALP production of MC3T3-E1 much better than the rest of the investigated fibrous substrates. Between the two types of the fibrous substrates, the one from 10 wt% PCL/PHBV solution was able to support the ALP production of the cells slightly better than the one from 12 wt% PCL solution (based on the basis of the average values of the obtained results.

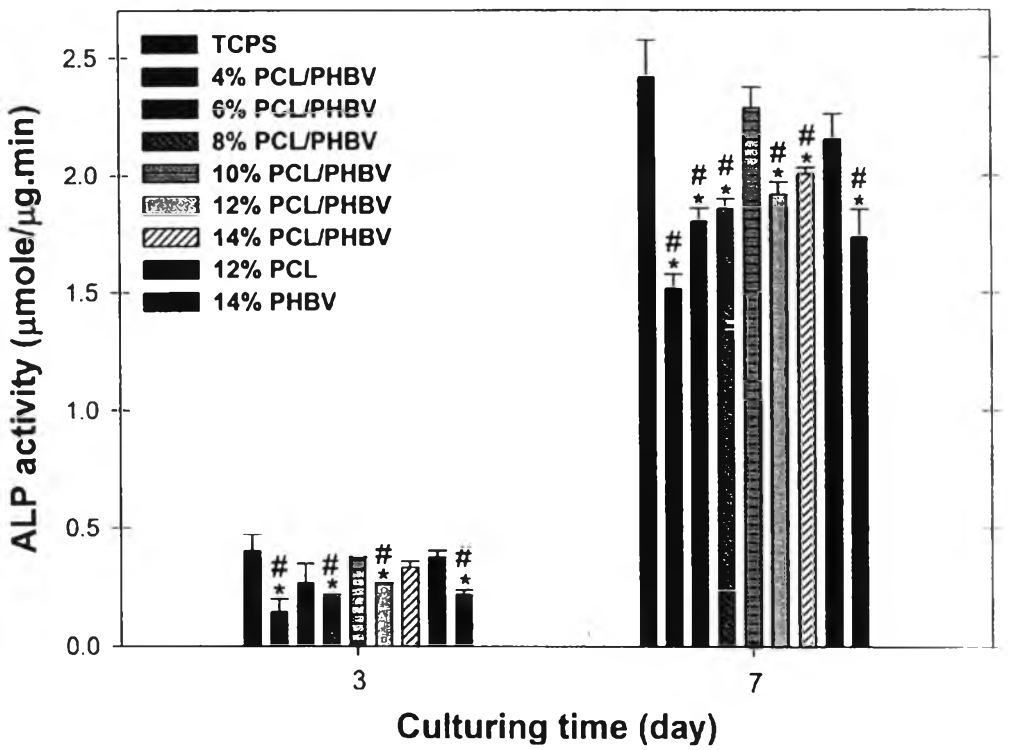

Figure 6.6 ALP activity of MC3T3-E1 that were cultured on the surfaces of TCPS and various types of the fibrous substrates at various time points after cell culturing. *Significance at $p < 0.05$ with respect to TCPS. #Significance at $p < 0.05$ with respect to the fibrous substrate from 12 wt% PCL solution.

6.4.4 Mineralization

The ability to promote the bone formation is the utmost important character of a bone scaffold. Here, photographic images of Alizarin Red S staining of MC3T3-E1 that had been cultured on TCPS and all types of the fibrous substrates for 14 days, along with their quantitative analyses, are shown in Figure 6.7. Due to the presence of calcium ions in the mineralized tissues, the staining product with Alizarin Red S appeared red. According to the obtained results, the cells that had been cultured on all types of the fibrous substrates stained positively for calcium deposition along with those that had been cultured on the fibrous substrate from 10 wt% PCL/PHBV solution exhibiting the greatest intensity, followed by those that had been cultured on the fibrous scaffold from 12 wt% PCL solution. Interestingly, despite the high attachment, high proliferation, and high expression of ALP for the

cells that had been grown on TCPS, mineralization of the cells on this control surface on day 14 was the lowest.

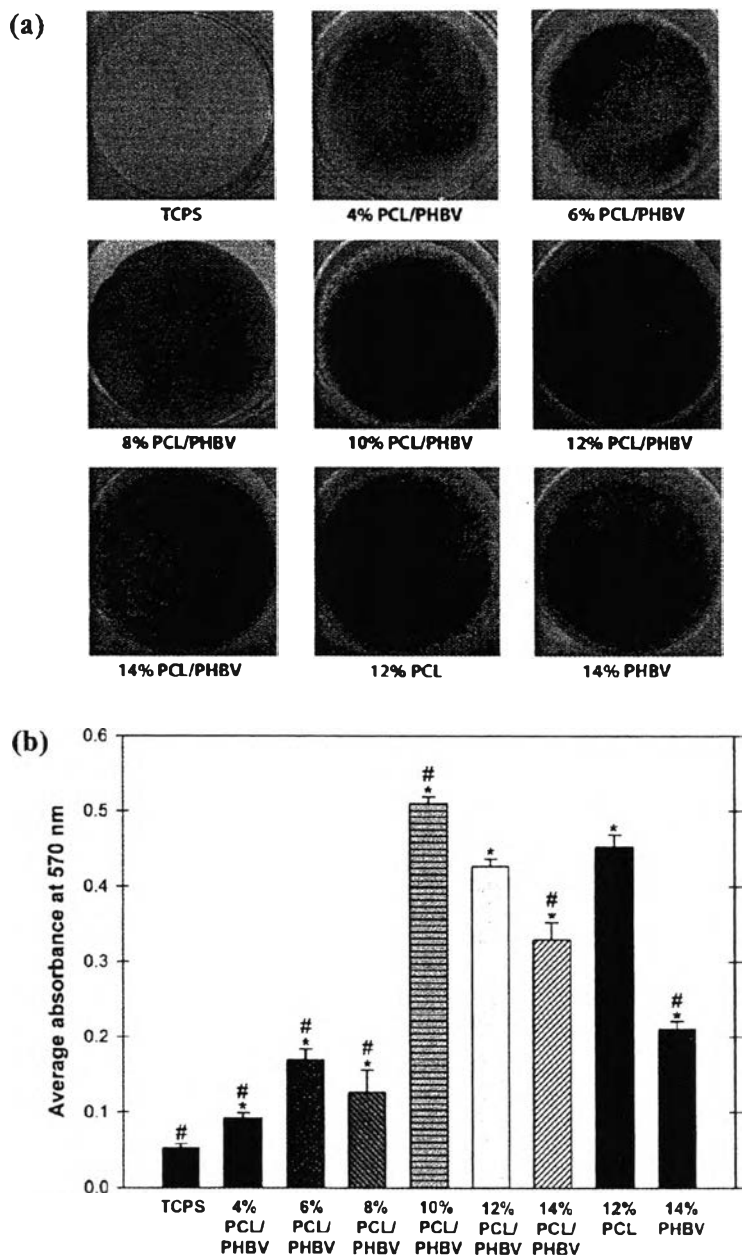

Figure 6.7 Alizarin Red S staining for mineralization of MC3T3-E1 on day 14 after being cultured on the surfaces of TCPS and various types of the fibrous substrates: (a) photographic images of the stained specimens and (b) the corresponding quantitative analyses. *Significance at $p < 0.05$ with respect to TCPS. #Significance at $p < 0.05$ with respect to the fibrous substrate from 12 wt% PCL solution.

All of the obtained results emphasize the importance of thorough investigation for the efficacy of a bone scaffold, as the mineralization of the bone cells does not depend totally on the ability of the scaffold in promoting the attachment, the proliferation, and/or the secretion of ALP of the cells. The obtained results also imply that both the topography (i.e., patterning and/or roughness) and the physicochemical characteristic (i.e., hydrophilicity/hydrophobicity) of the surface of a scaffold are important factors determining the efficacy of the scaffolds. To this end, it should also be emphasized that before a scaffold that has been evaluated as positive for promoting infiltration, attachment, proliferation, and differentiation of the target cells *in vitro* can be used *in vivo*, it should also be tested for inflammatory reactions because it has recently been demonstrated that *in vitro* inflammatory response of a scaffold by macrophages is also surface-topography-dependent (Saino *et al.*, 2011).

6.5 Conclusions

The fibrous substrates with different morphologies of the individual fibers were prepared from solutions of 50/50 w/w PCL/PHBV in 80/20 v/v chloroform/DMF by electrospinning. As the concentration of the solutions increased from 4 to 14 wt%, the topography of the individual fibers changed from discrete beads/smooth fibers, to beaded fibers/smooth fibers, and finally to smooth fibers and the size of the individual fibers increased from ~0.4 to ~1.8 μm on average. Among the various fibrous substrates, the one prepared from 10 wt% PCL/PHBV solution exhibited the lowest static water contact angles of ~85° on average. Likely because of the smoothness of the obtained fibrous substrate and the lowest water contact angles of its surface, the fibrous substrate from 10 wt% PCL/PHBV solution, with the average fiber diameter of ~0.8 μm, was the best at promoting the attachment, proliferation, and differentiation of the cultured mouse bone cells (MC3T3-E1). This type of fibrous matrix could be used as scaffolding substrates for calvarial defects.

6.6 Acknowledgments

The authors acknowledge the partial support received from 1) The Thailand Research Fund (TRF, grant no.: DBG5280015), 2) The Institute for the Promotion of Teaching Science and Technology (IPST, for the doctoral scholarship of P.K.), 3) The Petroleum and Petrochemical College (PPC), Chulalongkorn University, and 4) Center of Excellence on Petrochemical and Materials Technology (PETRO-MAT), Chulalongkorn University.

6.7 References

Bölgen, N., Menceloğlu, Y.Z., Acatay, K., Vargel, I., and Pişkin, E. (2005) *In vitro* and *in vivo* degradation of non-woven materials made of poly(ε-caprolactone) nanofibers prepared by electrospinning under different conditions. Journal of Biomaterials Science, Polymer Edition, 16, 1537-1555.

Cheng, S., Chen, G.Q., Leski, M., Zou, B., Wang, Y., and Wu, Q. (2006) The effect of *D*,*L*-β- hydroxybutyric acid on cell death and proliferation in L929 cells. Biomaterials, 27, 3758-3765.

Choi, J.Y., Lee, B.H., Song, K.B, Park, R.W., Kim, I.S., Sohn, K.Y., Jo, J.S., and Ryoo, H.M. (1996) Expression patterns of bone-related proteins during osteoblastic differentiation in MC3T3-E1 cells. Journal of Cellular Biochemistry, 61, 609-618.

Chuenjitkuntaworn, B., Inrung, W., Damrongsri, D., Mekaapiruk, K., Supaphol, P., and Pavasant, P. (2010) Polycaprolactone/hydroxyapatite composite scaffolds: preparation, characterization, and *in vitro* and *in vivo* biological responses of human primary bone cells. Journal of Biomedical Materials Research Part A, 94, 241-251.

Gassner, F. and Owen, A.J. (1996) Some properties of poly(3-hydroxybutyrate-*co*-3-hydroxyvalerate) blends. Polymer International, 39, 215-219.

Holmes, P.A. (1985) Applications of PHB: a microbially-produced biodegradable thermoplastic. Physics in Technology, 16, 32-36.

Ito, Y., Hasuda, H., Kamitakahara, M., Ohtsuki, C., Tanihara, M., Kang, I.K., and Kwon, O.H. (2005) A composite of hydroxyapatite with electrospun biodegradable nanofibers as a tissue engineering material. Journal of Bioscience and Bioengineering, 100, 43-49.

Kenar, H., Torun Köse G., and Hasirci V. (2006) Tissue engineering of bone on micropatterned biodegradable polyester films. Biomaterials, 27, 885-895.

Kenawy, E.R., Layman, J.M., Watkins, J.R., Bowlin, G.L., Matthews, J.A., Simpson, D.G., and Wnek, G.E. (2003) Electrospinning of poly(ethylene-*co*-vinyl alcohol) fibers. Biomaterials, 24, 907-913.

Khang, G., Lee, S.J., Lee, J.H., Kim, Y.S., and Lee, H.B. (1999) Interaction of fibroblast cells on poly(lactide-co-glycolide) surface with wettability chemogradient. Bio-Medical Materials and Engineering, 9, 179-187.

Kumbar, S.G., Nukavarapu, S.P., James, R., Nair, L.S., and Laurencin, C.T. (2008) Electrospun poly(lactic acid-co-glycolic acid) scaffolds for skin tissue engineering. Biomaterials, 29, 4100-4107.

Li, W.J., Laurencin, C.T., Caterson, E.J., Tuan, R.S., and Ko, F.K. (2002) Electrospun nanofibrous structure: a novel scaffold for tissue engineering. Journal of Biomedical Materials Research Part A, 60, 613-621.

Ndreu, A., Nikkola, L., Ylikauppila, H., Ashammakhi, N., and Hasirci, V. (2008) Electrospun biodegradable nanofibrous mats for tissue engineering. Nanomedicine, 3, 45-60.

Noh, H.K., Lee, S.W., Kim, J.M., Oh, J.E., Kim, K.H., Chung, C.P., Choi, S.C., Park, W.H., and Min, B.M. (2006) Electrospinning of chitin nanofibers: degradation behavior and cellular response to normal human keratinocytes and fibroblasts. Biomaterials, 27, 3934-3944.

Oh, S.H., Park, I.K., Kim, J.M., and Lee, J.H. (2007) *In vitro* and *in vivo* characteristics of PCL scaffolds with pore size gradient fabricated by a centrifugation method. Biomaterials, 28, 1664-1671.

Qiu, Z., Yang, W., Ikehara, T, and Nishi, T. (2005) Miscibility and crystallization behavior of biodegradable blends of two aliphatic polyesters. Poly(3-hydroxybutyrate-*co*-3-hydroxyvalerate) and poly(ε-caprolactone). Polymer, 46, 11814-11819.

Rivard, C.H., Chaput, C., Rhalmi, S., and Selmani, A. (1996) Polyesters biosynthétiques absorbables et regénération tissulaire. Étude de la prolifération tri-dimensionnelle de cellules orthopédiques. Annales de Chirurgie, 50, 651-658.

Saino, E., Focarete, M.L., Gualandi, C., Emanuele, E., Cornaglia, A.I., Imbriani, M., and Visai, L. (2011) Effect of electrospun fiber diameter and alignment on macrophage activation and secretion of proinflammatory cytokines and chemokines. Biomacromolecules, 12, 1900-1911.

Sangsanoh, P., Waleetorncheepsawat, S., Suwantong, O., Wutticharoenmongkol, P., Weeranantanapan, O., Chuenjitbuntaworn, B., Cheepsunthorn, P., Pavasant, P., and Supaphol, P. (2007) *In vitro* biocompatibility of Schwann cells on surfaces of biocompatible polymeric electrospun fibrous and solution-cast film scaffolds. Biomacromolecules, 8, 1587-1594.

Shor, L., Güçeri, S., Chang, R., Gordon, J., Kang, Q., Hartsock, L., An, Y., and Sun, W. (2009) Precision extruding deposition (PED) fabrication of polycaprolactone (PCL) scaffolds for bone tissue engineering. Biofabrication, 1, No. 015003.

Sombatmankhong, K., Suwantong, O., Waleetorncheepsawat, S., and Supaphol, P. (2006) Electrospun fiber mats of poly(3-hydroxybutyrate), poly(3-hydroxybutyrate-*co*-3- hydroxyvalerate) and their blends. Journal of Polymer Science Part B: Polymer Physics., 44, 2923-2933.

Sudesh, K., Abe, H., and Doi, Y. (2000) Synthesis, structure and properties of polyhydroxyalkonates: biological polyester. Progress in Polymer Science, 25, 1503-1555.

Taepaiboon, P., Rungsardthong, U., and Supaphol, P. (2006) Drug-loaded electrospun mats of poly(vinyl alcohol) fibres and their release characteristics of four model drugs. Nanotechnology, 17, 2317-2329.

Thomson, R.C., Wake, M.C., Yaszemski, M.J., and Mikos, A.G. (1995) Biodegradable polymer scaffolds to regenerate organs. Advances in Polymer Science, 122, 245-274.

Tong, H.W., Wang, M., and Lu, W. (2011) Electrospinning and evaluation of PHBV-based tissue engineering scaffolds with different fibre diameters,

surface topography and compositions. Journal of Biomaterials Science, Polymer Edition. DOI: 10.1163/092050611X560708.

Tuzlakoglu, K., Bolgen, N., Salgado A.J., and Gomes, M.E. (2005) Nano- and microfiber combined scaffolds: a new architecture for bone tissue engineering. Journal of Materials Science: Materials in Medicine, 16, 1099-1104.

Varnell, D.F., Runt, J.P., and Coleman, M.M. (1981) Fourier transform infrared studies of polymer blends. 6. Further observations on the poly(bisphenol A carbonate)-poly(ε-caprolactone) system. Macromolecules, 14, 1350-1356.

Wang, B., Cai, Q., Zhang, S., Yang, X., and Deng, X. (2011) The effect of poly(L-lactic acid) nanofiber orientation on osteogenic responses of human osteoblast-like MG63 cells. Journal of Mechanical Behavior of Biomedical Materials, 4, 600-609.

Wang, J., Valmikinathan, C.M., Liu, W., Laurencin, C.T., and Yu, X. (2010) Spiral-structured, nanofibrous, 3D scaffolds for bone tissue engineering. Journal of Biomedical Materials Research Part A., 93, 753-762.

Wutticharеonmongkol, P., Sanchavanakit, N., Pavasant, P., and Supaphol, P. (2006) Preparation and characterization of novel bone scaffolds based on electrospun polycaprolactone fibers filled with nanoparticles. Macromolecular Bioscience, 6, 70-77.

Yeo, A., Rai, B., Sju, E., Cheong, J.J., and Teoh, S.H. (2008) The degradation profile of novel, bioresorbable PCL-TCP scaffolds: an *in vitro* and *in vivo* study. Journal of Biomedical Materials Research Part A, 84, 208-218.

Yoon, Y.I., Moon, H.S., Lyoo, W.S., Lee, T.S., and Park, W.H. (2008) Superhydrophobicity of PHBV fibrous surface with bead-on-string structure. Journal of Colloid and Interface Science, 320, 91-95.

Zhang, Y., Lim, C.T., Ramakrishna, S., and Huang Z.M. (2005) Recent development of polymer nanofibers for biomedical and biotechnological applications. Journal of Materials Science: Materials in Medicine, 16, 933-946.